RSC Advances

RSC Publishing

PAPER

View Article Online
View Journal | View Issue

Cite this: *RSC Advances*, 2013, **3**, 1476

A coal desulfurization process *via* sodium metaborate electroreduction with pulse voltage using a boron-doped diamond thin film electrode†

Chenhua Shu, Tonghua Sun,* Jinping Jia, Ziyang Lou and Yafei Shen

Received 29th July 2012,
Accepted 14th November 2012

DOI: 10.1039/c2ra21604c

www.rsc.org/advances

A preliminary study was conducted on the coal desulfurization process *via* $NaBO_2$ electroreduction with pulse voltage using a boron-doped diamond (BDD) thin film electrode. It has been proved that $NaBO_2$ was converted into $NaBH_4$ by ^{11}B NMR. The factors that influence the conversion rate of $NaBO_2$ into $NaBH_4$ and coal desulfurization efficiency were investigated. Under the conditions of −1.5 V forward pulse voltage, +0.5 V reverse pulse voltage, 0.2 mol L^{-1} $NaBO_2$ concentration, 0.5 mol L^{-1} NaOH concentration, 2 s forward pulse duration, 1 s reverse pulse duration, 50 g L^{-1} coal concentration, 0.8 mmol L^{-1} $NiCl_2$ concentration and 2.5 h electrolytic time, a higher desulfurization efficiency (64%) was obtained compared with the common electrochemical desulfurization (ECDS) process using a Pt electrode. By analyzing and comparing the coal samples and electrolytes before and after desulfurization it was indicated that the removed S from the coal sample in the form of gaseous H_2S was mainly converted into Na_2S and Na_2S_x and boron (B) recycling was realized during coal desulfurization. Particularly, the combustion characteristics of coal were improved after desulfurization. Finally, the desulfurization mechanism was proposed. All these results indicated that the desulfurization process *via* $NaBO_2$ electroreduction with pulse voltage using a BDD thin film electrode is effective and highly promising for coal desulfurization.

1 Introduction

Sulfur dioxide (SO_2) emissions from coal combustion have been implicated as a cause of acid rain and other air pollution related problems which can cause enormous economic losses.[1] A number of physical, microbial and chemical (including chemical oxidative and chemical reductive) coal desulfurization methods have been reported. The physical processes can only remove a portion of pyritic sulfur but cannot remove organic sulfur.[2,3] The microbial desulfurization methods were usually not very effective.[4–6] Chemical oxidative desulfurization methods can remove most sulfurs, including inorganic and organic forms, but the methods destroy the macromolecular structure and properties of coal.[7–14] Compared with oxidative desulfurization (OD), reductive desulfurization (RD) has more incomparable advantages such as mild conditions and short processing time. Sodium borohydride is a good reducing agent in many industrial processes, which was used in sulfur removal from gasoline and coal recently.[15–19] But the price of sodium borohydride is very expensive due to the limited deposition of boron minerals. $NaBO_2$, the hydrolytic by-product of $NaBH_4$, is much cheaper and more stable. It is of great importance to recycle $NaBO_2$ into $NaBH_4$. Because electroreduction methods can realize the conversion of $NaBO_2$ into $NaBH_4$, it is a good conception to combine the $NaBO_2$ electroreduction (electrochemical process) with the $NaBH_4$ reduction (chemical process) for reductive desulfurization of coal to realize boron (B) recycling. Namely, $NaBO_2$ was converted into $NaBH_4$ by electroreduction and subsequently the generated $NaBH_4$ was converted into $NaBO_2$ again while it was used for the reductive desulfurization of coal. Then, the above two processes were repeated. B recycling can be realized at the same time as coal desulfurization. This process is an integration of electrochemical and chemical processes for reductive desulfurization (ECCRD). Based on this conception, some research has been done.[20,21] However, the shortcomings of lower desulfurization efficiency due to the lower conversion rate of $NaBO_2$ into $NaBH_4$ and the use of inappropriate electrodes remain. Thus, it is necessary to explore an effective method to improve the conversion rate of $NaBO_2$ into $NaBH_4$. Many studies on the electroreduction of $NaBO_2$ into $NaBH_4$ have been reported.[22–27] The electroreduction mechanism is as follows:

$$\text{Cathode: } BO_2^- + 6H_2O + 8e^- \rightarrow BH_4^- + 8OH^-,\quad E_{1/2} = -1.24\ \text{V (}vs.\text{ SHE)} \tag{1}$$

$$\text{Anode: } 4OH^- - 4e^- \rightarrow 2H_2O + O_2\uparrow,\ E_{1/2} = 1.229\ \text{V (}vs.\text{ SHE)} \tag{2}$$

School of Environmental Science and Engineering, Shanghai Jiaotong University, Dongchuan Road 800, Shanghai, 200240, People's Republic of China.
E-mail: sunth@sjtu.edu.cn

† Electronic supplementary information (ESI) available. See DOI: 10.1039/c2ra21604c

The above equations show that BO_2^- is reduced to BH_4^- at the cathode, but due to charge repulsion it is very difficult for the negatively charged BO_2^- to keep close to the surface of the cathode. Thus, the conversion rate of $NaBO_2$ into $NaBH_4$ is very low when constant voltage is applied. The pulse voltage is a forward pulse (cathodic pulse) followed by a reverse pulse (anodic pulse), which means that the working electrode will turn into the anode after working for a period of time as the cathode. When the working electrode works as the anode, the negative charged BO_2^- will be attracted to the surface of the working electrode, and then the working electrode works as the cathode, the BO_2^- gathered on the surface of the working electrode will be reduced immediately into BH_4^- before being excluded. Afterwards, the directions of pulse voltage continue alternating, which means that the attraction and electroreduction of BO_2^- alternates on the working electrode. Thus, the conversion rate of $NaBO_2$ into $NaBH_4$ will be improved greatly by supplying pulse voltage.

In previous studies,[20,21] Pb electrodes were mainly used as the cathode in ECCRD processes. However, Pb was not a perfect cathode material due to its narrow potential window, high background current *etc.* Furthermore, Pb electrodes were prone to corrosion in strongly alkaline solution. The voltages for ECCRD processes were above 2 V and the Pb electrodes wore down after working for a period of time in previous studies. In recent years, the boron-doped diamond (BDD) film has been considered a very promising electrode material. It possesses several advantageous properties such as excellent chemical stability, high electrical conductivity, a wide potential window and low background current.[28–33] In this study the BDD film electrode was used as the working electrode for several reasons. Above all, the hydrogen evolution reaction ($2H_2O + 2e^- \rightarrow H_2\uparrow + 2OH^-$) might take place at the same time when the electroreduction of $NaBO_2$ proceeded. The BDD film electrode was capable of inhibiting the hydrogen evolution reaction due to its low potential of hydrogen evolution. Likewise, its high potential of oxygen evolution can avoid the oxygen evolution reaction ($4OH^- - 4e^- \rightarrow 2H_2O + O_2\uparrow$) when the reverse pulse was supplied (Fig. S1, ESI†).[31,34–36] Besides, its corrosion resistance makes it stable in strongly alkaline solution and its low background current is beneficial to improving current efficiency.

In this paper, in order to improve the desulfurization efficiency, the electroreduction of $NaBO_2$ into $NaBH_4$ was fulfilled with pulse voltage using a BDD thin film electrode. The factors that influence the conversion rate of $NaBO_2$ into $NaBH_4$ and the desulfurization efficiency were investigated. Furthermore, the results were compared with the common electrochemical desulfurization (ECDS) using a Pt electrode. Finally, the desulfurization was proposed by analysing and comparing the coal samples and electrolytes before and after desulfurization.

2 Experimental

2.1 Materials

A coal sample was collected from Zunyi, Guizhou province, China, which was ground and passed through a 140 mesh sieve. The proximate and ultimate analyses of coal sample are given in Table 1. A BDD thin film electrode was prepared by a hot filament

Table 1 Characterization of the coal samples

		Treated coal		
			ECDS[b]	
Parameters	Original coal	ECCRD[a]	ECODS	ECRDS
Ultimate analysis (wt%, db)				
C	71.27	69.29(−2.8%)	65.24(−8.4%)	69.37(−2.7%)
H	6.04	7.13	5.21	6.94
N	1.02	0.84	0.95	0.81
S	6.16	2.21(−64.1%)	2.69(−56.3%)	3.98(−35.4%)
$O_{diff.}$	15.51	20.53	25.91	18.9
Sulfur content of different forms (wt%, db)				
Pyritic sulfur (PS)	1.93	0.35(−81.9%)	0.39(−83.4%)	1.07(−44.6%)
Sulfate sulfur (SS)	0.57	0.12(−78.9%)	0.11(−80.7%)	0.34(−40.3%)
Organic sulfur $(OS)_{diff.}$	3.66	1.74(−52.5%)	2.19(−40.1%)	2.57(−29.8%)
Combustion characteristic				
Calorific value (J g^{-1})	24 267	24 703(+1.8%)	20 187(−16.8%)	24 089(−0.7%)
Ignition (T/°C)	483	473(−10)	476(−7)	478(−5)
Proximate analysis (wt%, db)				
Ash	20.1	13.8(−31.3%)	25.3(+25.8%)	18.6(−7.5%)
Volatile matter	8.2	6.5	8.5	7.5
Moisture[c]	1.6	1.4	1.5	1.4
Fixed $carbon_{diff.}$	70.1	78.3(+11.7%)	64.7(−7.7%)	72.5(+3.4%)

[a] Process conditions: −1.5 V forward pulse voltage, +0.5 V reverse pulse voltage, 0.2 mol L^{-1} $NaBO_2$ concentration, 0.5 mol L^{-1} NaOH concentration, 2 s forward pulse duration, 1 s reverse pulse duration, 50 g L^{-1} coal concentration, 0.8 mmol L^{-1} $NiCl_2$ concentration, 2.5 h electrolytic time. [b] Process conditions: 1 mol L^{-1} NaOH concentration, 50 g L^{-1} coal concentration, 2.5 V *vs.* SCE constant voltage. [c] Atmospheric conditions.

chemical vapor deposition (HFCVD) technique on tantalum substrate from acetone and hydrogen mixtures. Trimethyl borate served as the boron source. $NaBO_2 \cdot 4H_2O$ (>99%, AR), NaOH (>96%, AR) and $NiCl_2 \cdot 6H_2O$ (>98%, AR) were purchased from Sinopharm Chemical Reagent Co. Ltd. (Shanghai China).

2.2 Electroreduction of $NaBO_2$ into $NaBH_4$ experiment

As shown in Fig. 1(a), the electroreduction was carried out in an electrolytic cell with a cation exchange membrane separating the working electrode and the counter electrode compartments. An aqueous solution containing NaOH and a mixed aqueous solution containing NaOH and $NaBO_2$ were added into the counter electrode and working electrode compartments, respectively. The cation exchange membrane does not allow BO_2^- or BH_4^- to transfer to the counter electrode compartment so as to maintain a high concentration of BO_2^- near the working electrode, which prevents the electrooxidation of BH_4^- and BO_2^- on the working electrode. A BDD thin film electrode (40 × 10 mm) was used as the working electrode (WE). The counter electrode (CE) was a graphite electrode (40 × 10 mm). The reference electrode (RE) was a saturated calomel electrode and all the experimental potentials reported were normalized to this reference electrode. Pulse voltages were obtained from an electrochemical workstation (Autolab PGSTAT30) with PC software control (GPES 4.9). The generated $NaBH_4$ was analyzed by iodometric titration and ^{11}B nuclear magnetic resonance. The conversion rate of $NaBO_2$ into $NaBH_4$ was calculated by the following eqn (3), where C_1 (mol L^{-1}) is the $NaBO_2$ concentration in original electrolytes and C_2 (mol L^{-1}) is the $NaBH_4$ concentration in treated electrolytes.

$$\text{Conversation rate (\%)} = (C_2/C_1) \times 100\% \quad (3)$$

2.3 Coal desulfurization experiment by ECCRD process

As shown in Fig. 1(b), a magnetic stirrer and a gas pipeline for H_2S were added into the experimental setup of coal desulfur-

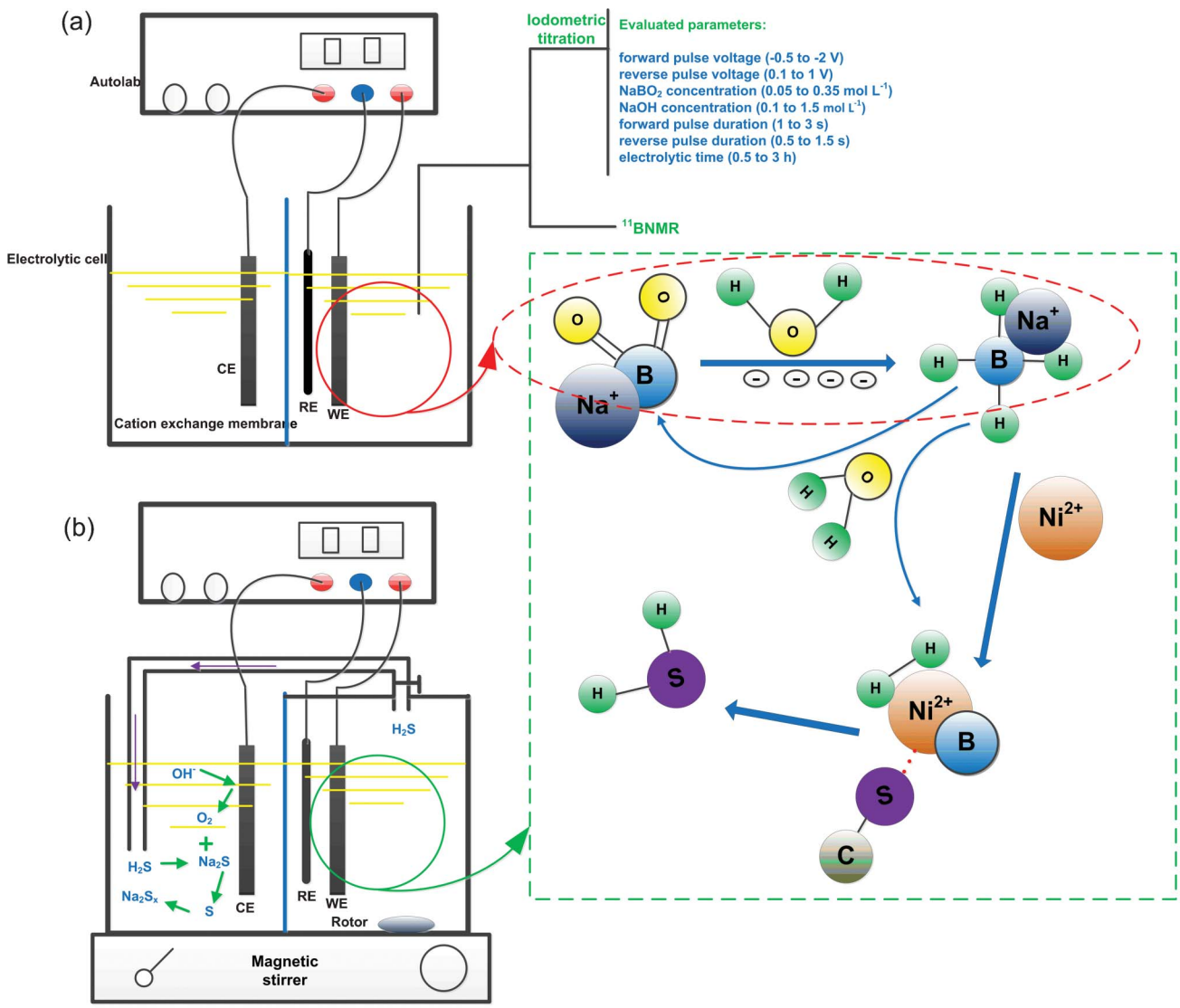

Fig. 1 Schematic diagram of electroreduction experiment (a) and coal desulfurization experiment by ECCRD process (b).

ization, compared with the experimental setup of electroreduction (Fig. 1(a)). In order to collect the generated H_2S, the WE compartment was sealed. First, an aqueous solution containing NaOH and a mixed aqueous solution containing NaOH and $NaBO_2$ were added into the CE and WE compartments, respectively. Meanwhile, the prepared coal sample and $NiCl_2$ catalyst were added into the WE compartment. Then, the magnetic stirrer and power were turned on in sequence and the reaction began immediately. After the end of the reaction the clean coal was obtained by filtering and leaching the coal slurry in the working compartment. At last, the clean coal sample and filtrate were used for s-content analysis and ICP analysis, respectively. Simultaneously the electrolytes in the counter compartment were also analyzed by ICP. The desulfurization efficiency was calculated by the following eqn (4), where TS_1 is the sulfur content in original coal samples and TS_2 is the sulfur content in treated coal samples.

$$\text{Desulfurization efficiency (wt\%)} = 1/TS_1\ (TS_1 - TS_2) \times 100\% \quad (4)$$

2.4 Coal desulfurization experiment by ECDS process

In order to compare with the ECCRD processes using BDD thin film electrodes, the common electrochemical desulfurization (ECDS) experiments were carried out using Pt electrodes. According to the desulfurization mechanism, ECDS prcesses can be divided into two categories: electrochemical oxidation desulfurization (ECODS) and electrochemical reduction desulfurization (ECRDS).[37] The ECDS experiments were carried out in an electrolytic cell with a cation exchange membrane separating the anodic and cathodic compartments. For the ECODS process, a Pt electrode (10 × 10 mm) was used as the anode and a graphite electrode (10 × 10 mm) was used as the cathode. For the ECRDS process, on the contrary, a Pt electrode (10 × 10 mm) was used as the cathode and a graphite electrode (10 × 10 mm) was used as the anode. Two aqueous solutions containing NaOH were added into the the anodic and cathodic compartments, respectively. Meanwhile, the prepared coal sample was added into the Pt electrode compartment. Then, the magnetic stirrer and power were turned on in sequence and the reaction began immediately. After the end of the reaction, the clean coal was obtained by filtering and leaching the coal slurry. At last, the clean coal samples were used for s-content analysis.

2.5 Analysis methods

Total sulfur (TS) was determined using an elemental analyzer (Elementar Vario EL III, Germany); sulfate sulfur (SS) was analyzed gravimetrically, using the Eschka method; pyritic sulfur (PS) was analyzed by measuring the amount of iron combined in the pyritic state (GB/T 215-2003); and organic sulfur (OS) was estimated by the difference. The proximate analysis of the coal sample followed the Chinese standard method (GB/T 212-2001). The analysis of calorific value and ignition temperature followed the Chinese standard methods (GB/T 213-2003) and (GB/T 18511-2001), respectively. The qualitative and quantitative detection of $NaBH_4$ was fulfilled by ^{11}B nuclear magnetic resonance (Bruker Avance III 400 NMR spectrometer, room temperature, 128 MHz) and iodometric titration.[38] The elemental analysis of electrolytes and filtrates was determined using an inductively coupled plasma (ICP, Iris Advantage 1000, Thermo King-CordCo., USA) instrument. The data was presented as the average of two replicates (data error <5%) in each treatment.

3 Results and discussion

3.1 Electroreduction of $NaBO_2$ into $NaBH_4$ process

3.1.1 Effect of forward pulse voltage, reverse pulse voltage, $NaBO_2$ concentration, NaOH concentration on conversion rate. *Forward pulse voltage.* The role of forward pulse voltage was to reduce BO_2^- into BH_4^-. According to the cyclic voltammograms of BDD thin film electrode (Fig. S1, ESI†), the reduction peak of $NaBO_2$ to $NaBH_4$ was observed at around −1.5 V. Although reducing the forward pulse voltage probably improved the conversion rate, too low a voltage would lead to hydrogen evolution reaction. Fig. 2(a) showed the effect of forward pulse voltage on conversion rate, compared with constant voltage. There was no $NaBH_4$ to generate when constant voltage was higher than −1.2 V; below that, the maximum value of conversion rate reached 6.28% at −1.8 V. However, when the pulse voltage was supplied, the maximum value was up to 15.33% at the forward pulse voltage of −1.5 V. The results suggest that the performance of pulse voltage electrolysis was significantly better than that of constant voltage electrolysis. When the forward pulse voltage was lower than −1.5 V the conversion rate decreased instead of increasing due to the hydrogen evolution reaction. Thus, −1.5 V was considered as the optimum value of forward pulse voltage.

Reverse pulse voltage. The role of reverse pulse voltage was to attract BO_2^- to the surface of BDD thin film electrode. A high reverse pulse voltage was beneficial for BO_2^- attraction to the BDD thin film electrode. However, the oxygen evolution reaction (Fig. S1, ESI†) and conversion of BO_2^- to borax[39] might take place when the reverse pulse voltage was too high. On the contrary, a low reverse pulse voltage was not enough to attract BO_2^- to the surface of the BDD thin film electrode. As shown in Fig. 2(b), the conversion rate initially increased with the increasing of reverse pulse voltage, and then decreased. The maximum value of conversion rate was obtained when the reverse pulse voltage was +0.5 V.

$NaBO_2$ concentration. $NaBO_2$ is the source of $NaBH_4$, so the concentration of $NaBO_2$ is a key factor of producing $NaBH_4$. As shown in Fig. 2(c), the conversion rate increased with the increasing of $NaBO_2$ concentration when the $NaBO_2$ concentration was less than 0.2 mol L^{-1}, but decreased when the $NaBO_2$ concentration was more than 0.2 mol L^{-1}. The reason was that the oxidation and hydrolysis of $NaBH_4$ intensified with the increase of concentration of $NaBH_4$. Namely, the total $NaBH_4$ concentration would remain constant while increasing to a certain value. According to eqn (3), the conversion rate would decrease with the increase of $NaBO_2$ concentration under constant $NaBH_4$ concentration. However, the maximum

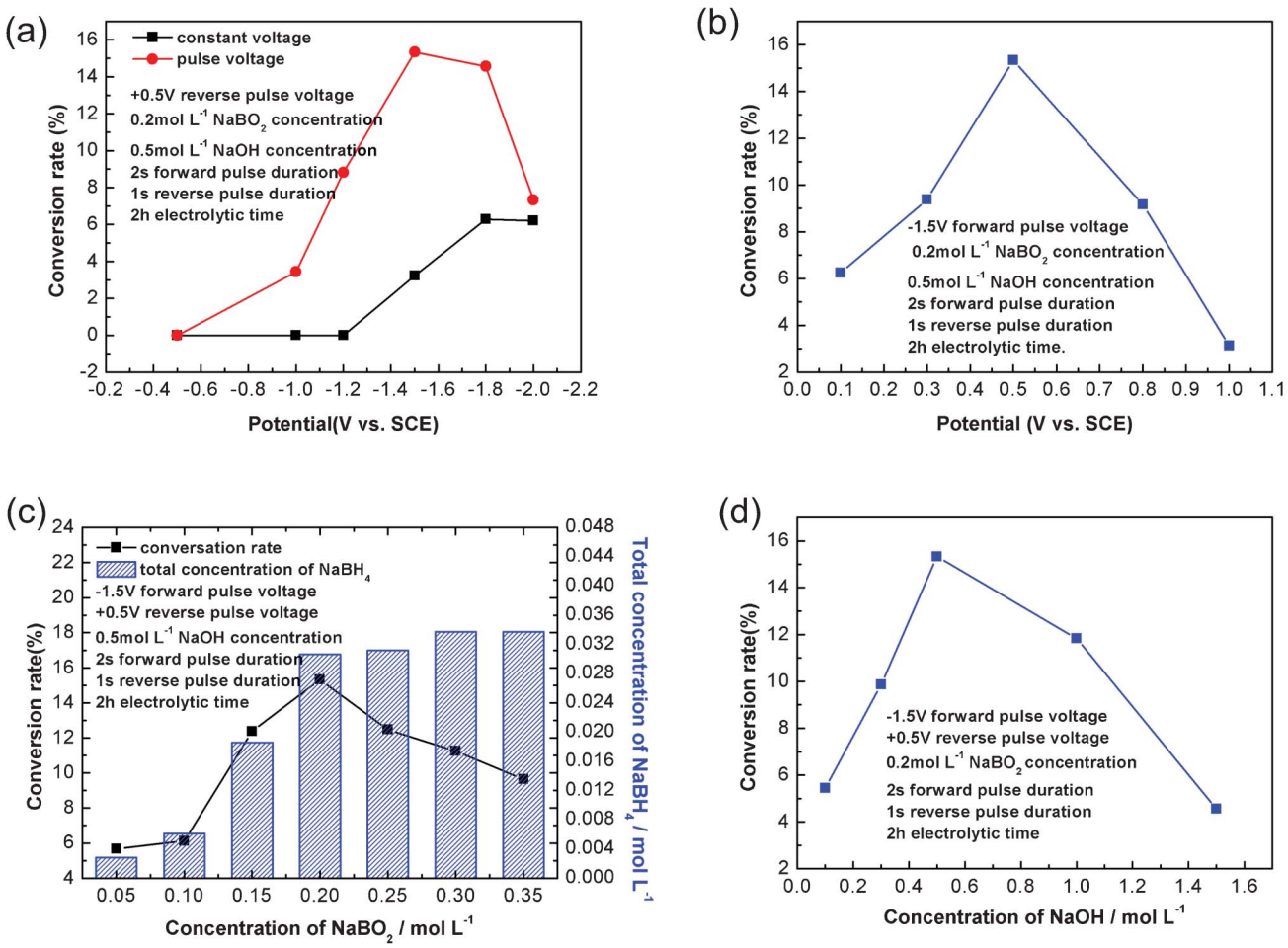

Fig. 2 Effect of forward pulse voltage (a), reverse pulse voltage (b), $NaBO_2$ concentration (c) and NaOH concentration (d) on conversion rate.

value of total $NaBH_4$ concentration can be observed at the $NaBO_2$ concentration of 0.3 mol L^{-1}. The 0.2 mol L^{-1} of $NaBO_2$ concentration was used in the following experiments.

NaOH concentration. There are two contradictory effects of increasing NaOH concentration. On the one hand, it is well known that $NaBH_4$ is unstable and hydrolyzes spontaneously when stored in aqueous solution. This hydrolysis reaction can be greatly inhibited by the addition of NaOH because $NaBH_4$ can be stable in the strong alkaline solutions. For example, when the pH is 8, more than 50% of $NaBH_4$ can hydrolyze within 30 s. However, the half-life of $NaBH_4$ is 430 d when the pH is 14.[40] On the other hand, increasing NaOH concentration can reduce the potential of oxygen evolution reaction, which makes it easier for oxygen evolution to take place when a reverse pulse voltage is supplied. Furthermore, increasing NaOH concentration can improve the viscosity of electrolyte, which makes it difficult for BO_2^- to transfer to the surface of the BDD thin film electrode. Thus, it was necessary to investigate a reasonable NaOH concentration for the electrochemical reduction. As shown in Fig. 2(d), the conversion rate increased initially, and then decreased with the increase of NaOH concentration. The maximum value of conversion rate was obtained when the NaOH concentration was 0.5 mol L^{-1}.

3.1.2 Effect of forward pulse duration, reverse pulse duration and electrolytic time on conversion rate. The role of forward pulse voltage was to reduce $NaBO_2$ to $NaBH_4$. Increasing the forward pulse duration can improve the conversion rate within a certain range, but if the forward pulse duration is too long, the conversion rate would also decrease because pulse numbers would reduce under constant total electrolytic time. The role of reverse pulse voltage was to attract BO_2^- to the surface of the BDD thin film electrode. If the reverse pulse duration was too short, it wouldn't be enough to transfer BO_2^- to the surface of the BDD thin film electrode. Conversely, the conversion rate would also decrease because the electrooxidation of BO_2^- and BH_4^- would increase. Tables 2a and 2b presented the experimental and analytical results of the orthogonal array for the three factors. Obviously, the most important influence factor was the reverse pulse duration. However, the forward pulse duration had a lesser effect on the conversion rate. The optimum values of the forward and reverse pulse durations are 2 s and 1 s, respectively. Increasing the electrolytic time was evidently beneficial for improving the conversion rate, ranking only

Table 2 (a) Experimental design and results for electroreduction processes according to L_9 (3^3) orthogonal array[a]. (b) Data handling of the orthogonal array

Table 2a

Run no.	Forward pulse duration (s)	Reverse pulse duration (s)	Electrolytic time (h)	Conversion rate (%)
1	1	0.5	0.5	5.78
2	1	1	1	12.45
3	1	1.5	2	5.56
4	2	0.5	1	7.55
5	2	1	2	15.33
6	2	1.5	0.5	4.34
7	3	0.5	2	9.23
8	3	1	0.5	6.45
9	3	1.5	1	3.67

[a] Other reaction conditions: −1.5 V forward pulse voltage, +0.5 V reverse pulse voltage, 0.2 mol L^{-1} $NaBO_2$ concentration, 0.5 mol L^{-1} NaOH concentration.

Table 2b

V_i^b (%)	Parameters		
	Forward pulse duration(s)	Reverse pulse duration(s)	Electrolytic time(h)
V_1	7.930	7.52	5.523
V_2	9.073	11.41	7.89
V_3	6.45	4.523	10.04
Range	2.623	6.887	4.517

[b] V_i: average of the conversion rate at the same level; range = (V_i)max − (V_i)min.

second to the reverse pulse duration. To further validate the effect of electrolytic time, it was necessary to carry out some supplementary experiments (Fig. 3(b)).

3.1.3 Confirmation of electroreduction of $NaBO_2$ into $NaBH_4$ by ^{11}B NMR. The electrolytes before and after electroreduction were analyzed by ^{11}B NMR. Fig. 3(a) showed the results of ^{11}B NMR analysis. The resonance lines near 1.6 ppm can be assigned to $NaBO_2$[39] and those near 42 ppm can be assigned to $NaBH_4$[41] which appeared only in the electrolytes after electrochemical treatment. The result was in good agreement with the results of iodometric titration which suggested that $NaBH_4$ was obtained through the electroreduction of $NaBO_2$ using a boron-doped diamond thin film electrode with pulse voltage.

The electrolytic time is also of great importance to the conversion rate of $NaBO_2$ into $NaBH_4$. As shown in Fig. 3(b), the conversion rate increased before 2 h, after which the growth trend slowed down rapidly. Considering economic efficiency, 2 h was selected as the optimum value of electrolytic time.

3.2 Coal desulfurization process

3.2.1 Effect of coal concentration on desulfurization efficiency and total sulfur removal in the ECCRD process. Coal concentration has an effect on the mass transfer, and the

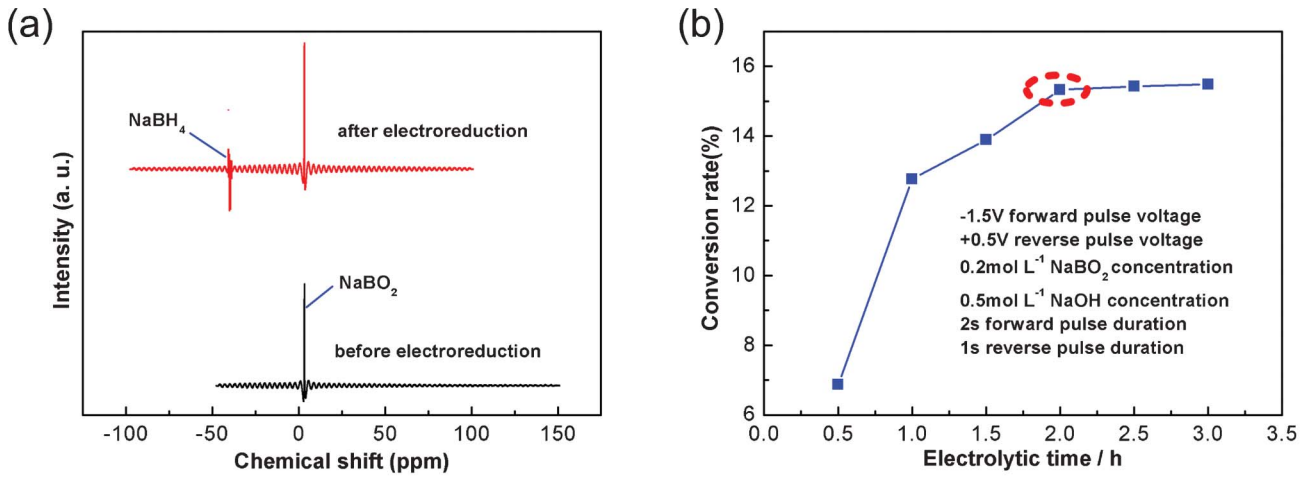

Fig. 3 ^{11}B NMR spectrogram of electrolytes before and after electroreduction, Process conditions: −1.5 V forward pulse voltage, +0.5 V reverse pulse voltage, 0.2 mol L^{-1} $NaBO_2$ concentration, 0.5 mol L^{-1} NaOH concentration , 2 s forward pulse duration, 1 s reverse pulse duration, 2 h electrolytic time (a). Effect of electrolytic time on conversion rate (b).

probability of contact with the active hydrogen atom (H*). Low coal concentration benefited mass transfer, but it decreased the contact frequency of H* and coal particles to some extent, resulting in the reduction of desulfurization efficiency. However, a high coal concentration inhibited mass transfer, which also decreases desulfurization efficiency. As shown in Fig. 4(a), the maximum value of desulfurization efficiency (64.1%) was observed at a coal concentration of 50 g L^{-1}, while the maximum value of total sulfur removal reached 2.08 g when the coal concentration was 60 g L^{-1}.

3.2.2 Effect of $NiCl_2$ concentration on desulfurization efficiency in the ECCRD process. It is well known that metal borides (*e.g.* NiB, CoB) are highly active catalysts which can be generated readily from metal halides (*e.g.* $NiCl_2$, $CoCl_2$) and boron hydrides (*e.g.* $NaBH_4$) in protic conditions.[42] Particularly, nickel borides have been employed as efficient and convenient reagents for reductive desulfurization.[43–46] In this work, in order to improve the desulfurization efficiency, $NiCl_2$ was added to enhance the reducibility of $NaBH_4$. As shown in Fig. 4(b), the desulfurization efficiency was still very low after electrolyzing for 5 h without $NiCl_2$. However, with the increasing of $NiCl_2$ concentration, the desulfurization efficiency increased and the treatment time decreased. When the $NiCl_2$ concentration increased to 0.8 mmol L^{-1}, the desulfurization efficiency and treatment time remained almost stable. The desulfurization efficiency was above 60% for 2.5 h electrolysis. The possible reason (Fig. 1) is that nickel borides were prepared by the reaction of $NiCl_2$ with $NaBH_4$ in protic solvents ($4NaBH_4 + 2NiCl_2 + 9H_2O \rightarrow Ni_2B + 3H_3BO_3 + 4NaCl + 12.5H_2\uparrow$).[47,48] Under the catalysis of nickel borides, $NaBH_4$ can immediately react with H_2O, producing amounts of H_2 (or active hydrogen). Then, the activated hydrogen was adsorbed on the surface of nickel borides (Ni–B), forming into a kind of Ni–MH intermediate product. On the other hand, the S atom in coal contains lone-pair electrons, and Ni^{2+} had an empty d-orbital, so S can react easily with Ni^{2+}. Finally, the highly activated hydrogen adsorbed on the surface of nickel boride (Ni–B) attacked S bonded with $^{\alpha}C$, resulting in C–S bond cleavage.[49,50]

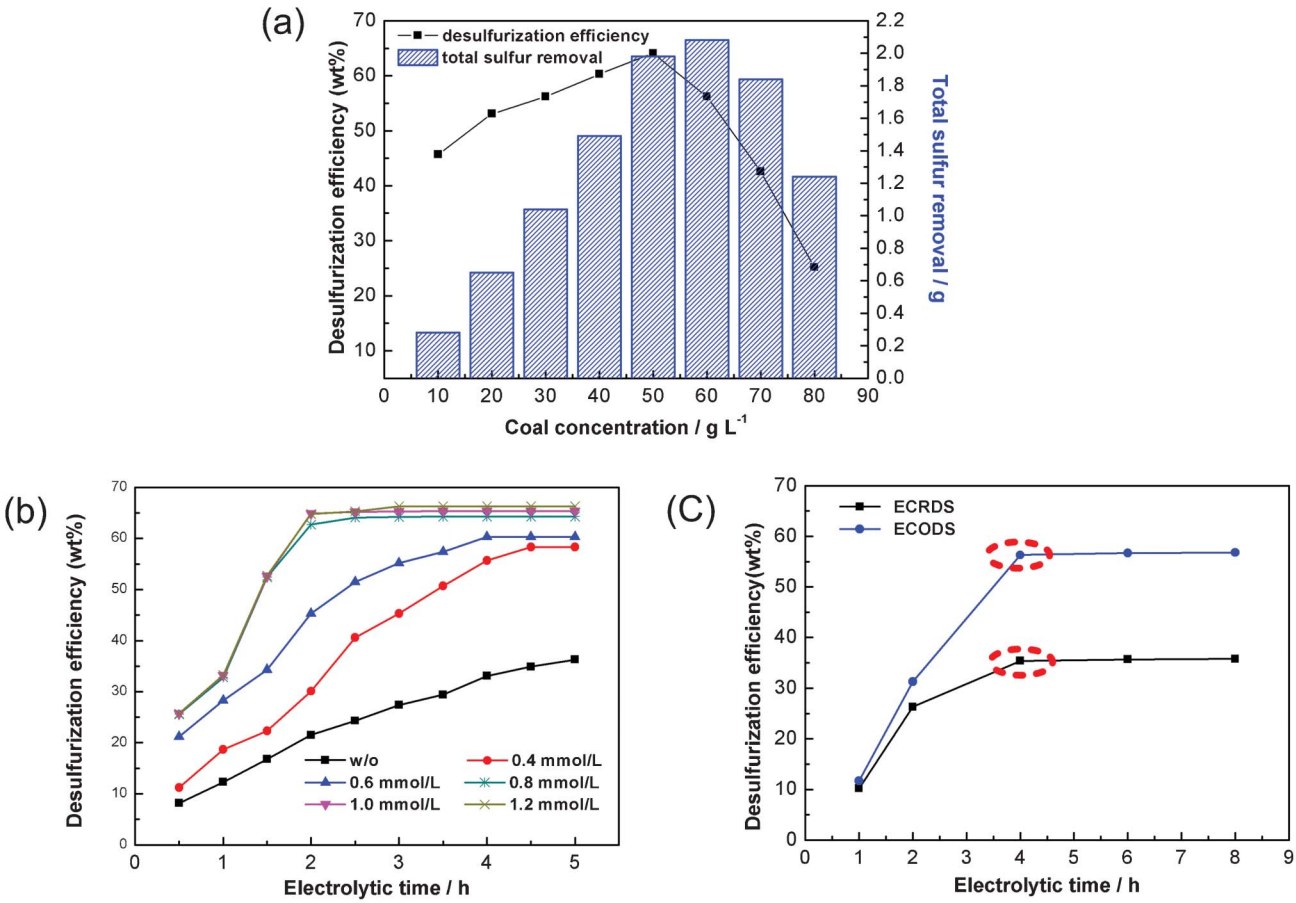

Fig. 4 Effect of coal concentration on desulfurization efficiency and total sulfur removal in the ECCRD process; other reaction conditions: −1.5 V forward pulse voltage, +0.5 V reverse pulse voltage, 0.2 mol L^{-1} $NaBO_2$ concentration, 0.5 mol L^{-1} NaOH concentration, 2 s forward pulse duration, 1 s reverse pulse duration, 0.8 mmol L^{-1} $NiCl_2$ concentration, 2.5 h electrolytic time (a). Effect of $NiCl_2$ concentration on desulfurization efficiency in the ECCRD process; other reaction conditions: −1.5 V forward pulse voltage, +0.5 V reverse pulse voltage, 0.2 mol L^{-1} $NaBO_2$ concentration, 0.5 mol L^{-1} NaOH concentration, 2 s forward pulse duration, 1 s reverse pulse duration, 50 g L^{-1} coal concentration (b). Effect of electrolytic time on desulfurization efficiency in the ECDS process; reaction conditions: 1 mol L^{-1} NaOH concentration, 50 g L^{-1} coal concentration, 2.5 V *vs.* SCE constant voltage (c).

3.2.3 Effect of electrolytic time on desulfurization efficiency. Fig. 4(b) also showed the effect of electrolytic time on desulfurization efficiency in the ECCRD process. The desulfurization efficiency increased rapidly with the increasing of electrolytic time when electrolytic time was less than 2 h, after which, the growth trend slowed down. The desulfurization efficiency reached more than 64% at 2.5 h of electrolytic time. Fig. 4(c) showed the effect of electrolytic time on desulfurization efficiency in the ECDS process. The maximum values of desulfurization efficiency (56.3% for the ECODS process and 35.4% for the ECRDS process) were obtained at 4 h of electrolytic time. In the same electrolytic time, the desulfurization efficiency by the ECODS process was obviously higher than that by the ECRDS process. In contrast to the ECRDS and ECODS processes, the ECCRD process improved the desulfurization efficiency in a shorter electrolytic time.

3.2.4 Mass balance in the ECCRD process. Table 3 presents the ICP analytical results of the filtrates from the working electrode compartment and the electrolytes from the counter electrode compartment. The mass of TS removal: experimental value (g L^{-1}) = desulfurization efficiency (wt%) × total sulfur content (wt%) × coal concentration (g L^{-1}) = 64.1% × 6.16% × 50 g L^{-1} = 2.12 g L^{-1}; estimated value (g L^{-1}) = S_1 (sulfur in the working electrode compartment, g L^{-1}) + S_2 (sulfur in the counter electrode compartment, g L^{-1}) = (0.95 + 1.11) = 2.06 g L^{-1}. Obviously, the estimated value of TS reduction is almost in accordance with its corresponding experimental value, which demonstrated that the removed S is practically converted into H_2S. After treatment, Ni and B were reduced from 0.047 to 0.043 g L^{-1} (by 8.5%), and from 2.16 to 2.12 g L^{-1} (by 1.8%), respectively. Thus, a large proportion of Ni and B could be recycled and reused.

3.2.5 Coal characterization. Calorific value and ignition temperature are two important combustion characteristics of coal. Oxidative desulfurization usually tended to decrease the calorific value due to carbon loss. However, the calorific value of coal can also increase after desulfurization because the desulfurization process can lead to its simultaneous demineralization.[51] Thus, how the calorific value changes after desulfurization may depend on the ratio of decarbonitation and demineralization.[52] Table 1 presents the changes of coal characteristics before and after desulfurization. For the ECCRD process, the efficiencies of decarbonization and deashing were 2.8 and 31.3%, respectively. The calorific value of the coal sample increased from 24 267 to 24 703 J g^{-1} (or by 1.8%). For the ECODS process, the efficiencies of decarbonization was 8.4%, but the ash content increased by 25.8%, so the calorific value decreased from 24 267 to 20 187 J g^{-1} (or by 16.8%). For the ECRDS process, the calorific value of the coal sample remained almost unchanged. After desulfurization, all three processes slightly lowered the ignition temperature of the coal samples. These results indicate that the desulfurization process by ECCRD is a relatively mild desulfurization method, because not only can it remove S but can also improve the combustion characteristics of coal.

3.3 Mechanism of coal desulfurization in the ECCRD process

According to previous reports in the literature[16–21] and the analysis of experimental results, the possible desulfurization mechanism was proposed as follows (eqn (1), (2) and (5)–(11) and Fig. 1):

$$\text{WE: } BO_2^- + 6H_2O + 8e^- \rightarrow BH_4^- + 8OH^- \quad (1)$$

$$BH_4^- + 2H_2O \rightarrow BO_2^- + 4H_2\ (H^*) \quad (5)$$

$$FeS_2 + 2H^* \rightarrow Fe + S + H_2S\uparrow \quad (6)$$

$$2H^* + R\text{–}SH \rightarrow R\text{–}H + H_2S\uparrow \quad (7)$$

$$4H^* + R\text{–}S\text{–}R' \rightarrow R\text{–}H + R'H + H_2S\uparrow \quad (8)$$

$$H_2S + 2NaOH \rightarrow Na_2S + 2H_2O \quad (9)$$

$$\text{CE: } 4OH^- - 4e^- \rightarrow 2H_2O + O_2\uparrow \quad (2)$$

$$H_2S + 2NaOH \rightarrow Na_2S + 2H_2O \quad (9)$$

$$2H_2O + 2Na_2S + O_2 \rightarrow 2S + 4NaOH \quad (10)$$

$$(x - 1)S + Na_2S \rightarrow Na_2S_x \quad (11)$$

As shown in the above eqn (1), (2) and (5)–(11) and Fig. 1, the removed S in the form of gaseous H_2S from the coal sample was mainly converted into Na_2S and Na_2S_x. B recycling was realized at the same time of coal desulfurization. Thus, the ECCRD process reduced the additional pollution and realized

Table 3 ICP analytical results of filtrates and electrolytes[a]

Compartment	Element	Before reaction[b] (g L^{-1})	After reaction(g L^{-1})
Working electrode compartment	S	0	0.95
	Fe	0	0.35
	Na	16.1	15.9
	Ni	0.047	0.028
	B	2.16	2.12
Counter electrode compartment	S	0	1.11
	Fe	0	0.28
	Na	11.5	10.8
	Ni	0	0.015

[a] Process conditions: −1.5 V forward pulse voltage, +0.5 V reverse pulse voltage, 0.2 mol L^{-1} NaBO2 concentration, 0.5 mol L^{-1} NaOH concentration, 2 s forward pulse duration, 1 s reverse pulse duration, 0.8 mmol L^{-1} NiCl2 concentration, 50 g L^{-1} coal concentration, 2.5 h electrolytic time. [b] Theoretical value.

the reasonable application and sustainable development of resources which only used electricity and green solutions (B recycling by electrolysis).

4 Conclusions

Electrochemical synthesis of $NaBH_4$ with pulse voltage using a BDD thin film electrode and its application to coal desulfurization was presented in this work. The results of iodometric titration and ^{11}B NMR suggested that $NaBH_4$ was obtained through the electrochemical reduction of $NaBO_2$. The factors that influenced the conversion rate of $NaBO_2$ into $NaBH_4$ and coal desulfurization efficiency were investigated. Under the conditions of −1.5 V forward pulse voltage, +0.5 V reverse pulse voltage, 0.2 mol L^{-1} $NaBO_2$ concentration, 0.5 mol L^{-1} NaOH concentration, 2 s forward pulse duration, 1 s reverse pulse duration, 50 g L^{-1} coal concentration, 0.8 mmol L^{-1} $NiCl_2$ concentration and 2.5 h electrolytic time, the desulfurization efficiency reached more than 64%. In contrast with the ECRDS and ECODS processes, the ECCRD process improved the desulfurization efficiency with a lower voltage and in a shorter electrolytic time. By analyzing and comparing the coal samples and electrolytes before and after desulfurization it was indicated that the removed S from coal sample in the form of gaseous H_2S was mainly converted into Na_2S and Na_2S_x and that B recycling was realized simultaneous to coal desulfurization. Additionally, after desulfurization, the combustion characteristics of coal were improved and the BDD thin film electrode remained nearly intact. Finally, the desulfurization mechanism was proposed. In summary, the coal desulfurization process *via* sodium metaborate electroreduction with pulse voltage using a BDD thin film electrode is effective and highly promising, which will open up new possibilities for coal desulfurization.

Acknowledgements

This work is financially supported by the National Key Technology R&D Program (No. 2010BAK69B24) and the National Natural Science Foundation of China (No. 41173108).

References

1 C. F. You and X. C. Xu, *Energy*, 2010, **35**, 4467–4472.
2 P. K. Naik, P. S. R. Reddy and V. N. Misra, *Fuel Process. Technol.*, 2004, **85**, 1473–1485.
3 Z. F. Luo, Y. M. Zhao, Q. R. Chen, M. M. Fan and X. X. Tao, *Fuel Process. Technol.*, 2002, **79**, 63–69.
4 C. Aacharya, R. N. Kar and L. B. Sukla, *Fuel*, 2001, **80**, 2207–2216.
5 C. Aacharya, L. B. Sukla and V. N. Misra, *Fuel*, 2005, **84**, 1597–1600.
6 H. He, F. F. Hong, X. X. Tao, L. Li, C. Y. Ma and Y. D. Zhao, *Fuel Process. Technol.*, 2012, **101**, 73–77.
7 K. C. Chaung, R. Markuszewesky and T. D. Wheelock, *Fuel Process. Technol.*, 1983, **7**, 43–57.
8 R. A. Rodriguez, C. C. Jul and D. G. Limon, *Fuel*, 1996, **75**, 606–612.
9 S. Mukherjee, S. Mahiuddin and P. C. Borthakur, *Energy Fuels*, 2001, **15**, 1418–1424.
10 R. Alvarez, C. Clemente and D. Gomez-Limon, *Fuel*, 2003, **82**, 2007–2015.
11 K. Charutawai, S. Ngamprasertsisith and P. Prasassarakich, *Fuel Process. Technol.*, 2003, **84**, 207–216.
12 W. D. Li and E. H. Cho, *Energy Fuels*, 2005, **19**, 499–507.
13 B. P. Baruah, B. K. Saikia, P. Kotoky and P. G. Rao, *Energy Fuels*, 2006, **20**, 1550–1555.
14 H. G. Alam, A. Z. Mohaddam and M. R. Omidkhah, *Fuel Process. Technol.*, 2009, **90**, 1–7.
15 Z. X. Wang, S. J. Wang, G. Y. Liu and W. B. Wang, *Pet. Process. Petrochem.*, 2007, **38**, 6–9.
16 Z. L. Li, T. H. Sun and J. P. Jia, *Fuel Process. Technol.*, 2010, **91**, 1162–1167.
17 Y. F. Shen, T. H. Sun and J. P. Jia, *Energy Fuels*, 2011, **25**, 2963–2967.
18 Y. F. Shen, T. H. Sun and J. P. Jia, *RSC Adv.*, 2012, **2**, 3123–3132.
19 Y. F. Shen, T. H. Sun and J. P. Jia, *RSC Adv.*, 2012, **2**, 4189–4197.
20 Y. F. Shen, X. L. Yang, T. H. Sun and J. P. Jia, *Energy Fuels*, 2011, **25**, 5007–5014.
21 Y. F. Shen, T. H. Sun and J. P. Jia, *Fuel*, 2012, **96**, 250–256.
22 G. F. Hu, F. Chapel, A. D. Mceiroy, E. City and R. M. Adams, *US Pat.*, 2 855 353, 1958.
23 H. B. H. Cooper, *US Pat.*, 3 734 842, 1973.
24 H. Sharifian and J. S. Dutcher, *US Pat.*, 4 904 357, 1990.
25 C. H. Hale and H. Sharifian, *US Pat.*, 4 931 154, 1990.
26 S. Amendola, *US Pat.*, 6 497 973 B1, 2002.
27 A. E. Sanli, İ. Kayacan, B. Z. Uysal and M. L. Aksu, *J. Power Sources*, 2010, **195**, 2604–2606.
28 M. Panizza and G. Cerisola, *Electrochim. Acta*, 2005, **51**, 191–199.
29 C. Saez, M. Panizza, M. A. Rodrigo and G. Cerisola, *J. Chem. Technol. Biotechnol.*, 2007, **82**, 575–581.
30 M. Panizza and A. Kapalka, *Electrochim. Acta*, 2008, **53**, 2289–2295.
31 M. Panizza and G. Cerisola, *Chemosphere*, 2009, **77**, 1060–1064.
32 S. C. Elaoud, M. Panizza, G. Cerisola and T. Mhiri, *J. Chem. Technol. Biotechnol.*, 2012, **87**, 381–386.
33 G. M. Swain and R. Ramesham, *Anal. Chem.*, 1993, **65**, 345–351.
34 H. B. Martin, A. Argoitia, U. Landau, A. B. Anderson and J. C. Angus, *J. Electrochem. Soc.*, 1996, **143**, L133–L136.
35 M. C. Granger, M. Witek, J. S. Xu, J. Wang, M. Hupert, A. Hanks, M. D. Koppang, J. E. Butler, G. Lucazeau, M. Mermoux, J. W. Strojek and G. M. Swain, *Anal. Chem.*, 2000, **72**, 3793–3804.
36 D. A. Tryk, K. Tsunozaki, T. N. Rao and A. Fujishima, *Diamond Relat. Mater.*, 2001, **10**, 1804–1809.
37 V. Lam, G. C. Li, C. J. Song, J. W. Chen, C. Fairbridge, R. Hui and J. J. Zhang, *Fuel Process. Technol.*, 2012, **98**, 30–38.
38 D. A. Lyttle, E. H. Jensen and W. A. Struck, *Anal. Chem.*, 1952, **24**, 1843–1844.

39 E. H. Park, S. U. Jeong, U. H. Jung and S. H. Kim, *Int. J. Hydrogen Energy*, 2007, **32**, 2982–2987.
40 W. Rong, *J. Fudan Univ (Nat Sci)*, 1998, **37**, 276–278.
41 S. Garroni, C. Milanese, D. Pottmaier, G. Mulas, P. Nolis, A. Girella, R. Caputo, D. Olid, F. Teixdor, M. Baricco, A. Marini, S. Surinach and M. Dolors, *J. Phys. Chem. C*, 2011, **115**, 16664–16671.
42 B. Ganem and J. O. Osby, *Chem. Rev.*, 1988, **86**, 763–780.
43 J. M. Khurana, A. Ray and S. Singh, *Tetrahedron Lett.*, 1998, **39**, 3829–3832.
44 J. M. Khurana, G. Kukreja and G. Bansal, *J. Chem. Soc., Perkin Trans. 1*, 2002, 2520–2524.
45 J. M. Khurana and G. Kukreja, *J. Heterocycl. Chem.*, 2003, **40**, 677–679.
46 J. M. Khurana and D. Magoo, *Synth. Commun.*, 2010, **40**, 2908–2913.
47 T. G. Back, J. K. Yang and H. R. Krouse, *J. Org. Chem.*, 1992, **57**, 1986–1990.
48 T. G. Back, D. L. Baron and K. Yang, *J. Org. Chem.*, 1993, **58**, 2407–2413.
49 J. C. Walter, A. Zurawski, D. Montgomery, M. Thornburg and S. Revankar, *J. Power Sources*, 2008, **179**, 335–339.
50 S. Schouten, D. Pavlović, J. S. Sinninghe Damsté and J. W. de Leeuw, *Org. Geochem.*, 1993, **19**, 901–909.
51 B. P. Baruah and P. Khare, *Energy Fuels*, 2007, **21**, 2156–2164.
52 K. C. Liu, J. Yang, J. P. Jia and Y. L. Wang, *Chemosphere*, 2008, **71**, 183–188.